COUPLED CONTAGION DYNAMICS OF FEAR AND DISEASE: MATHEMATICAL AND COMPUTATIONAL EXPLORATIONS

Joshua M. Epstein*,
Jon Parker**,
Derek Cummings***,
Ross A. Hammond**

October, 2007

"The plague was nothing; fear of the plague was much more formidable."
Henri Poincare

ABSTRACT: We model two interacting contagion processes: one of disease and one of *fear of*[1] the disease. Individuals can "contract" fear through contact with individuals who are infected with the disease (the sick), infected with fear only (the scared), and infected with both fear and disease (the sick and scared). Scared individuals--whether sick or not--may remove themselves from circulation with some probability, which affects the contact of individuals and thus the disease epidemic proper. If we allow individuals to recover from fear and return to circulation, the coupled dynamics become quite rich, and include multiple waves of infection, such as occurred in the 1918 flu pandemic. We also study flight as a behavioral response. In a spatially extended setting, even relatively small levels of fear-inspired flight can have a dramatic impact on spatio-temporal epidemic dynamics.

Keywords: mathematical epidemiology, agent-based models, contagion dynamics.

* Center on Social and Economic Dynamics, The Brookings Institution; External Professor, Santa Fe Institute; Visiting Professor, University of Pittsburgh School of Public Health.
** Center on Social and Economic Dynamics, The Brookings Institution
***The Johns Hopkins University Bloomberg School of Public Health.

[1] We do not define the term "fear." Readers should feel free to interpret it as "concerned awareness," for example. The point is that it is a behavior-inducing transmissible signal distinct from the pathogen itself. For expository purposes, "fear" will do.

Motivation

In classical mathematical epidemiology,[2] individuals do not adapt their contact behavior during epidemics. They do not endogenously engage, for example, in social distancing (protective sequestration) based on disease prevalence. Rather, they simply continue mixing (often uniformly) as if no epidemic were under way. This may be a reasonable assumption for non-lethal infections such as the common cold, but for lethal diseases such as AIDS, it is known to fail; and for other lethal disease threats, like pandemic influenza or bioterror smallpox, it seems likely to. People may be expected to adapt their contact patterns, and this will feed back to alter epidemic dynamics.

Homo EconomSickus

Economists have begun to address this issue, introducing the notion of *prevalence elastic behavior* into epidemic models. For example, as AIDS prevalence grows in a community, people may reduce their number of sexual partners. On prevalence elastic partner selection in AIDS, for example, see Kremer (1996). Predictably, *economic epidemiology*, as this subfield is called, posits optimizing behavior on the part of individuals. In effect, it models how canonically rational individuals would behave given some level of disease prevalence. They behave as *homo economicus* would behave given the associated health risks and costs of protection (e.g., vaccine-seeking). A term used for the resulting dynamics is *rational epidemics*. This literature includes elegant mathematical work, and captures—in the notion of prevalence elasticity—a clearly important phenomenon.

Boundedly Rational Epidemics

However, prevalence is treated as a kind of exogenous signal (suspiciously like a perfectly competitive price) to which agents respond with some elasticity. They do not interact directly with one another to gain information on prevalence or in deciding how to behave. The approach, therefore, seems ill-suited to capture cases where *endogenous epidemics of fear inspire widespread adaptations unrelated to prevalence*. Such cases abound: in 1996, millions of Indians fled Surat province to escape pneumonic plague. Yet, not a single case of pneumonic plague was actually confirmed. Prevalence of the disease itself, in other words, was zero. The model developed here handles cases where the fear is contagious, even though the pathogen is not (e.g., anthrax). Indeed, it handles cases where the event in question is not a pathogen at all, such as a chemical or radiological event, or natural disaster, such as an earthquake or volcano.

A second problem with the literature is that, even models that *do* include prevalence-dependent behavior assume behavioral changes that are *depressive* in their effect on the epidemic - protective self-isolation (sequestration) being the most common. However, research on mass behavior during crises (and even epidemics specifically) records another behavioral response that is common -

---

[2] This is the tradition of ordinary differential equations with perfect mixing (mass action kinetics) beginning with the 1927 Kermack-McKendrick model, which still dominates mathematical epidemiology (see Murray 1989, Anderson and May 1991).

flight. Unlike protective sequestration, flight has the potential to *increase* long-range mixing across spatial regions, exacerbating epidemics. In the model introduced here, we expand the behavioral response repertoire of agents infected with fear to include both flight and protective self-isolation.

In summary, most infectious disease modeling ignores behavior. Models have begun to include prevalence elastic behavior. It typically damps the epidemic. We introduce a model where fear and pathogen are coupled. Fear can spread independent of prevalence. In a spatially extended variant, flight is added to the behavioral repertoire. The full model can generate multi-wave dynamics, and elegantly shows how even a small amount of flight can amplify epidemic severity. To begin, we present the no-flight version.

PART I: THE BASIC NO FLIGHT MODEL

For expository purpose, we imagine two *contagion* processes: one of disease proper, and one of *fear about* the disease.[3] Individuals contract disease only through contact with the disease-infected (the sick). However, individuals can contract fear through contact with the disease-infected (the sick), the fear-infected (the scared, or worried well), or those infected with both fear and disease (the sick and scared). Scared individuals—whether sick or not—may withdraw from circulation with some probability, and return to circulation having recovered from fear, all of which affects the course of the disease epidemic proper.

Agents can occupy one and only one of seven states at any time. The model's (seven dimensional) state space is shown in Figure 1.

S:	Susceptible to pathogen and fear
I_F:	Infected with fear only
I_P:	Infected with pathogen only
I_{PF}:	Infected with pathogen and fear
R_F:	Removed from circulation due to fear
R_{PF}:	Removed from circulation due to fear and infected with pathogen
R:	Recovered from pathogen and immune to fear

Figure 1: *Possible States*

Let β denote the per-contact disease transmission rate, and let α denote the per-contact fear transmission rate. If we now imagine a susceptible individual (i.e., neither sick nor scared) having contact with one who is both sick and scared, then the transmission rates of fear, infection, and various combinations are given in Table 1. For instance, the probability that the first individual (neither sick nor scared) contracts neither bug nor fear is $(1-\alpha)(1-\beta)$, and so forth.

---

[3] As noted, the model in fact does not require that the disease be contagious—or for that matter, that the event which sparks the fear epidemic be a disease of any sort. It could be a radiological event, the DC snipers, 9/11, or an earthquake. We will return to these forms of the model.

	Get scared	Not get scared
Get sick	$\alpha \beta$	$(1 - \alpha) \beta$
Not get sick	$\alpha (1 - \beta)$	$(1 - \alpha)(1 - \beta)$

Table 1: Transmission Probabilities

Finally we specify parameters controlling the rate at which individuals self-isolate due to fear and recover from fear and return to circulation. These are given in Figure 2.

λ_1: Rate of removal to self-isolation of those infected with fear only
λ_2: Rate of recovery from infection with pathogen
λ_3: Rate of removal to self-isolation of those infected with fear and pathogen
H: Rate of recovery from fear and return to circulation

Figure 2: Parameters governing Removal and Return

With all of this in place, the model can be implemented as a classical well-mixed ordinary differential equation (ODE) system. The appropriate generalization of the standard Kermack-McKendrick (1927) ODE set-up is diagrammed in Figure 3 and formalized in the equations listed in Figure 4. The initial agent-based model will closely mimic these well-mixed differential equations. Each representation will inform the other. Having examined the well-mixed no-flight models in some detail, we will extend the agent model to better represent space, enabling the study of fear-inspired flight.
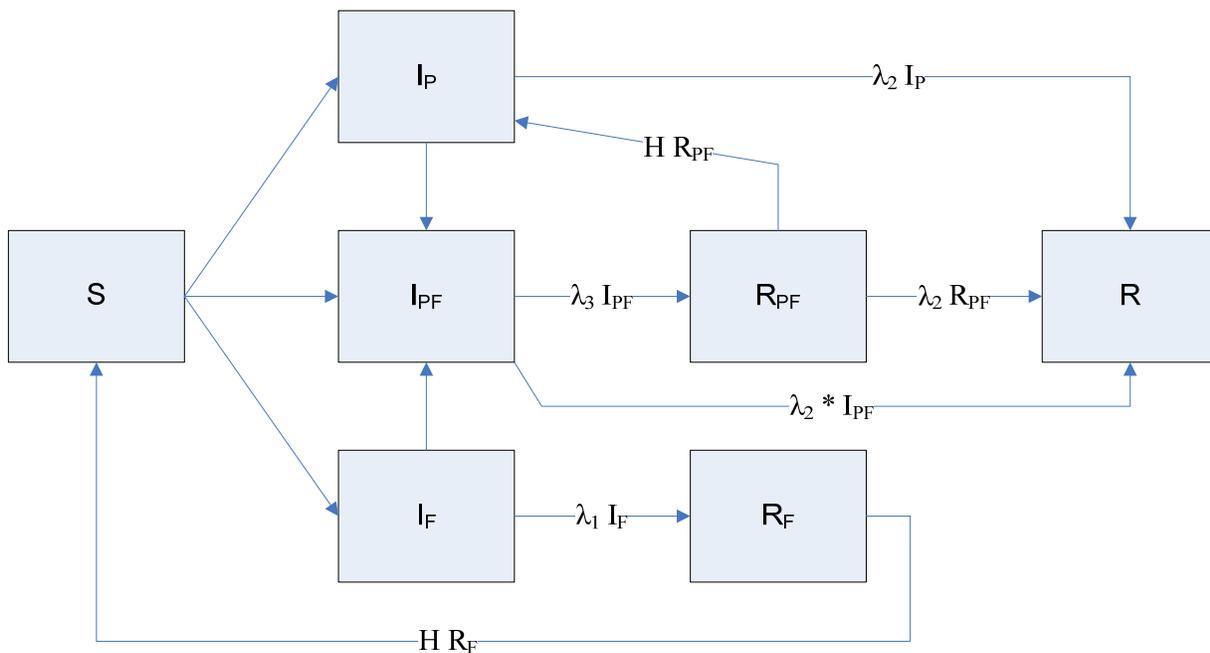

Figure 3: State transition chart.

$$\frac{dS}{dt} = -\beta(1-\alpha)SI_P - (1-\beta)\alpha SI_P - \beta\alpha SI_P - \alpha SI_F - \beta(1-\alpha)SI_{PF}$$
$$\qquad\qquad - (1-\beta)\alpha SI_{PF} - \beta\alpha SI_{PF} + HR_F$$

$$\frac{dI_F}{dt} = (1-\beta)\alpha SI_P + \alpha SI_F + (1-\beta)\alpha SI_{PF} - \beta I_F I_P - \beta I_F I_{PF} - \lambda_1 I_F$$

$$\frac{dI_P}{dt} = \beta(1-\alpha)SI_P + \beta(1-\alpha)SI_{PF} - \alpha I_P I_P - \alpha I_P I_F - \alpha I_P I_{PF} - \lambda_2 I_P + HR_{PF}$$

$$\frac{dI_{PF}}{dt} = \beta\alpha SI_P + \beta\alpha SI_{PF} + \beta I_F I_P + \beta I_F I_{PF} + \alpha I_P I_P + \alpha I_P I_F + \alpha I_P I_{PF} - \lambda_2 I_{PF} - \lambda_3 I_{PF}$$

$$\frac{dR_F}{dt} = \lambda_1 I_{PF} - HR_F$$

$$\frac{dR_{PF}}{dt} = \lambda_3 I_{PF} - \lambda_2 R_{PF} - HR_{PF}$$

$$\frac{dR}{dt} = \lambda_2 I_P + \lambda_2 I_{PF} + \lambda_2 R_{PF}$$

Figure 4: *Classical SIR Differential Equations Formulation*

Tracing through some simple state transitions, individuals susceptible to the Bug and Fear, *S*, flow into the Infected (with pathogen only) pool I_P at rate $\beta(1-\alpha)SI_P$ and into the pool infected with fear only I_F at rate $(1-\beta)\alpha SI_P$. Similarly, those who self-isolated out of fear only, denoted R_F (removed through Fear) return to the *S* pool at rate $H R_F$, where *the constant H* would yield exponential decay of individual fear, *ceteris paribus.* Clearly this most elementary form of the model assumes constant population; all the right-hand sides sum to zero.

While the differential equation form has the advantage of considerable elegance (exploited below to derive analytical expressions for R_0), there are some important extensions that are more naturally studied in agent-based models. For example, one mechanism for the multiple waves of 1918 was the premature government decisions to lift social distancing measures which were effective at reducing transmission. In many cities of the US, imposed bans on public gatherings, the closure of schools, and other measures meant to reduce transmission of influenza, were lifted once cases appeared to be at a minimum. Several cities prematurely declared victory over the epidemic and abruptly ended control measures. These edicts produced sharp step-functional returns from isolation and, as show below, these could have produced the multiple waves. In *linear* differential equation models step-functional forcings are elegantly handled through the use of Laplace Transform methods. But for the *nonlinear* equations above, these methods are not available, and numerical simulation is normally required. Agent-based models accommodate these step-functional forcings very naturally, and are developed next.

We will then extend this agent model to a version with both self-isolation and long-range flight. Of course, one could in principle formulate this as a high dimensional meta-population ODE model with many patches and coupling

coefficients.[4] However, with the inclusion of both self-isolation and flight, the result would be a fairly opaque ODE system. The agent version will prove very transparent, and quickly yields the main result: *even a small level of flight can dramatically affect contagion dynamics*. The next step, then, is to present the agent version of the ODE model presented above, and exercise it on some basic cases.

Agent-Based Computational Model

We retain the same seven pools enumerated above, and the qualitative flow chart of Figure 3. While local interactions are easily introduced, we will assume for exposition that agents move to random sites on a 200 X 200 site lattice with periodic boundary conditions (i.e., a torus). The agent population is 8000. When an agent moves to a new location, it interacts with a randomly selected Moore neighbor (agents on all eight neighboring sites), if such exists. Simulations begin with a single infected agent, so I(0) = 1.   Given a contact, transmissions of fear and disease are governed by α and β, defined earlier. For this basic version, the progression of random agent locations and neighbors is intended to mimic the well-mixed contact dynamics of the classical model.

Runs with Fear and Disease Uncoupled

The first elementary run of the model (Figure 5) posits no removal from circulation, either by fear (clamped at zero) or by disease (e.g., by morbidity or mortality), and no recovery from either the diseased or fear states. This is the classical SI case, and agrees with the special case of our general ODE model, á la Kermack-McKendrick.   S falls, I rises in familiar S-curves.
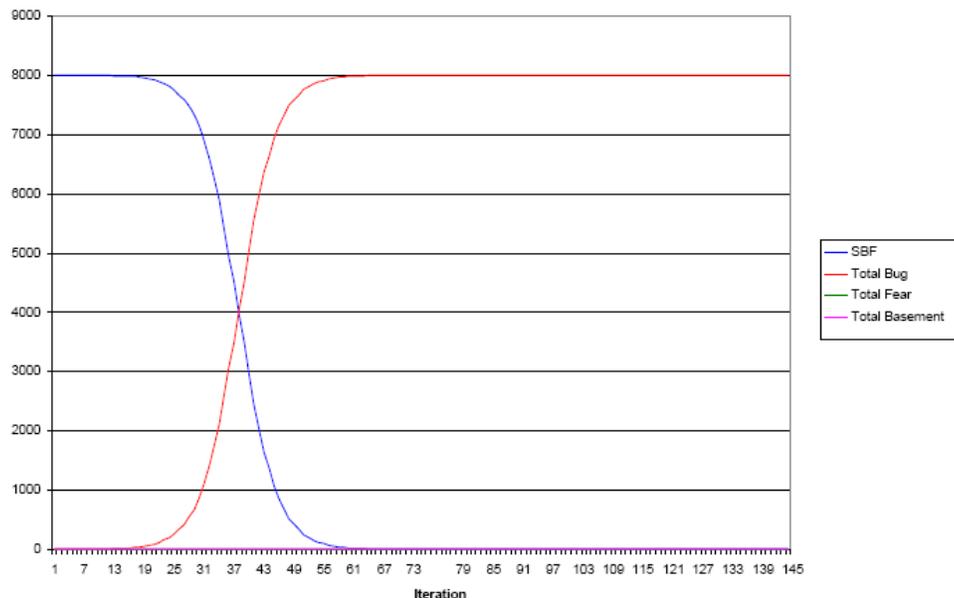

Figure 5: *Run 1. Pure Bug, No Fear, No Removal (α=0, β=.04)*

---

[4] Formulation as a reaction diffusion system on a spatial continuum might also be possible.

In Run 2, we reverse things, setting bug transmission (*β*) to zero, and fear transmission (*α*) to a positive value. We seed the simulation with a single case of fear rather than disease. Predictably, we generate a pure fear epidemic with no underlying disease. The Salem Witch Hunt would be an example, though, tragically, there are innumerable further ones. Analogous to the first Run, all susceptibles transfer into the Fear pool, despite actual disease (Red) remaining at zero.
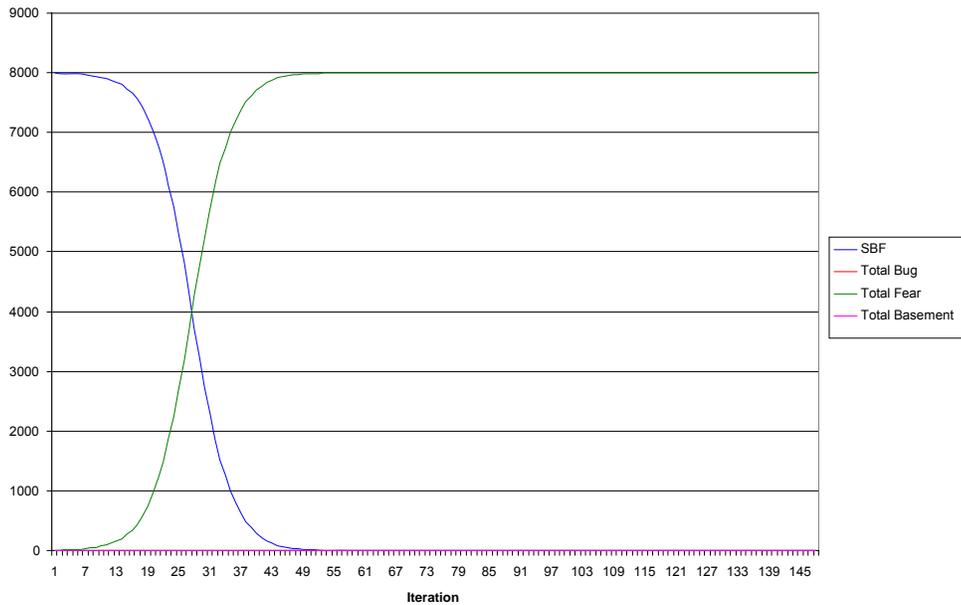

Figure 6*: Run 2. Salem Witches. Pure Fear (α=0.04), No Bug (β=0)*

Runs 1 and 2 seem reasonably predictable, and are symmetrical to one another: at *β*=.04 and *α* =0, we get one pair of S-curves. Reverse these settings (*β*=0, *α* =.04) and we get the reverse pair. Surely one would expect that if we set *α*=*β*=.04, the two epidemic S-curves should coincide. Is this what happens? Surprisingly, Run 3 shows the answer to be no (see Figure 7).

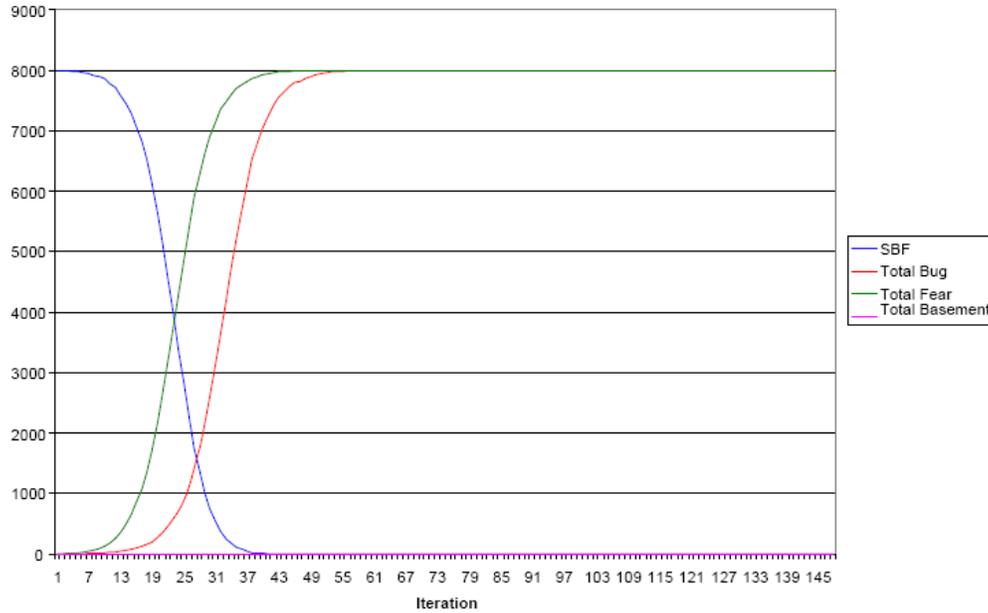**Figure 7**: Run 3. Coupled Case with α=β=0.04

The S-curves do *not* coincide   Indeed, *ceteris paribus*, the fear epidemic is faster then the bug epidemic. Why? The reason is that there are more pathways by which to contract fear than there are to contract bug. One can contract disease from contact with either of *two* pools: I_P or I_{PF}. But one can contract Fear by contact with any one of *three* pools: I_B, I_{BF}, or I_F. Obviously, once there is any fear, the latter three is a bigger set with which contact is more likely.

Insights from the Differential Equations: Reproductive Rates of Fear and Disease

Thus far, we have considered an SI model without recovery. The length of time for which people are transmissible with pathogen or fear greatly affects the speed at which epidemics progress. Since this agent model is essentially mimicking the differential equations, one might ask whether a classical analysis of those equations is illuminating on this point. One measure of speed is the basic reproduction number—the R_0, or "R-naught." This is defined as the expected number of secondary cases from a typical infectious individual during the entire period of their infectiousness in a completely susceptible population. The basic reproduction number of either the pathogen or fear can be found by calculating the spectral radius of the next generation operator. Diekmann et al. (1990) describe a procedure for estimating R_0 about the disease-free equilibrium. The basic reproduction number of the pathogen as a function of the transmission coefficient and rates of recovery or withdrawal from contact from the above system of equations is:

$$R_0(\text{pathogen}) = \frac{\beta(\lambda_2 + \lambda_3 - \alpha\lambda_3)}{\lambda_2(\lambda_2 + \lambda_3)} \quad [1]$$

8

Two types of individuals are infectious with the pathogen, I_P and I_{PF}. The average residence time in each of these states is $1/\lambda_2$ and $1/(\lambda_2+\lambda_3)$, respectively. Individuals in these states will infect others at a rate of β per unit time. R_0(pathogen) can be interpreted as a weighted sum of the product of β and the residence times in the two infectious states weighted by the fraction of those that become infected by the pathogen who transit to I_P $(1-\alpha)$ and I_{PF} (α). The basic reproduction number of fear is given by:

$$R_0(\text{fear}) = \max\left(\frac{\alpha}{\lambda_1}, \frac{\beta\alpha}{\lambda_2+\lambda_3}\right) \quad [2]$$

The first term above, α/λ_1, is the product of the transmission coefficient of fear, α, and the duration of the infectious period of fear, $1/\lambda_1$. This is the classical form of the basic reproductive number for a pathogen in a SIR model with a closed population. The second term dictates the growth of the fear epidemic when the length of time that individuals infected with both fear and pathogen are transmitting fear is longer than the length of time that people with just fear transmit the fear. The second term of [2] is greater than the first term only when the ratio of the infectious period of fear, $1/\lambda_1$ to the infectious period of those with pathogen and fear in this system $1/(\lambda_2+\lambda_3)$ is less than the transmission coefficient of the pathogen, β. In this case, the basic reproduction number of the pathogen always exceeds the basic reproduction number of fear.

In the case where $\alpha=\beta$ and $\lambda_1=\lambda_2=\lambda_3=\lambda$ we find, as we found in the simplified SI agent model, fear spreads faster than disease, as R_0 (fear)=α/λ > R_0(pathogen)= $\alpha/2\lambda$ (α and λ are both non-negative). When all three rate constants and the transmission coefficients differ from one another, the basic reproductive number of fear exceeds the basic reproductive number of the pathogen precisely when:

$$\alpha > \frac{\beta\lambda_1(\lambda_2+\lambda_3)}{(\lambda_1+\lambda_3)(\lambda_2+\lambda_3)-\beta\lambda_1\lambda_3} \quad [3]$$

In the absence of fear or pathogen, these models collapse to SIR or SIRS models in pathogen or fear. In the absence of transmissible fear, α =0, R_0(pathogen) [1] reduces to the classical R_0 of β/λ_3. In the absence of pathogen, the model collapses to an SIRS model of fear due to the recovery of individuals to the susceptible state and R_0(fear) is α/λ_1. Clearly, then, the coupled model subsumes the classical one.

In spatially extended settings where fear may inspire long-range migration, the possibility of fear propagating faster than bug will prove highly consequential. It may also generate high congestion undermining evacuation efforts and exacerbating exposures. Now we turn to 1918.

Explaining Multiple Waves of Infection in 1918: Bottom-Up and Top-Down Mechanisms

An outstanding question in epidemiology has been to account for the multiple temporal waves of incidence observed in the 1918 Pandemic Flu. Figure 8 shows the temporal mortality pattern due to influenza in four cities of the United States.
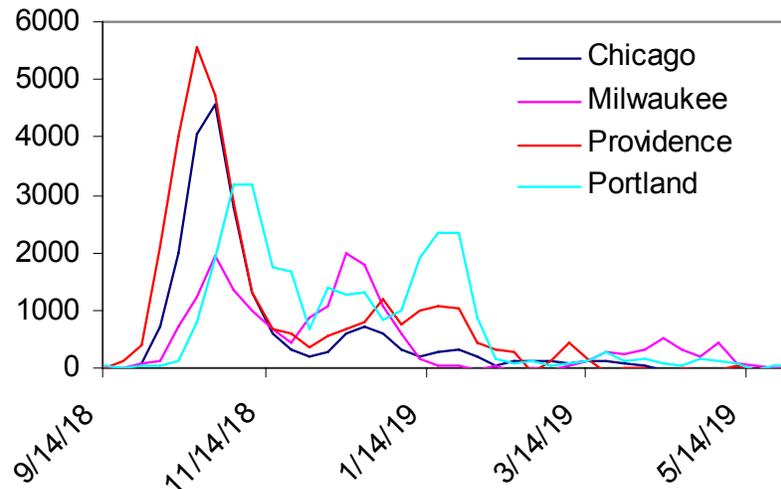

Figure 8: *Temporal Mortality Pattern*

It is clear from the statistical work of Louis (Yue, *et al.*, in prep) and others that no simple variation on the classical well-mixed differential equations will generate these waves. There has been elegant recent work adapting earlier ideas (Kremer, 1996) of prevalence elasticity to this important case (Bootsma and Ferguson, 2007). These authors have suggested that temporal waves in the incidence of influenza during the pandemic of 1918 were caused by behavioral responses to the pandemic which reduced contact, temporarily halting the increase of influenza infections. However, cases surged once again a few weeks after the initial peaks, once these behavioral adaptations were relaxed. Bootsma and Ferguson fit deterministic models to these patterns of multiple waves using *both* endogenous (bottom up) changes in contact rates *and* changes in contact rates due to (top down) edicts from central authorities. This does indeed generate multiple waves, and the authors have calibrated these impressively to the historical data. *But either mechanism alone is sufficient*, as we now show.

Endogenous Account in the ODE Model

The interaction of incidence of pathogen and fear of the pathogen can create temporal patterns with multiple peaks in the incidence of the infectious disease. An example is shown in Figure 9a. In this numerical simulation of the model, the incidence of the pathogen initially increases, then as the epidemic of fear increases, the number of susceptible individuals exposed to infectious individuals declines because many individuals remove themselves from circulation due to fear. This causes a temporary decline in the number of

individuals infected with the pathogen, but as individuals return (from removal) to the susceptible compartment having recovered from fear, transmission of the pathogen increases the number of individuals in I_P, creating a second peak in disease cases. Figure 9b shows a plot of the I_P compartment against the I_F, showing (i) the initial increase of both pathogen and fear from an initial state of I_P=0.001, I_F=0, (ii) a decrease in pathogen while fear continues to increase, (iii) the resurgence of the pathogen as fear decreases and finally, (iv) a decline of the pathogen prevalence to 0.
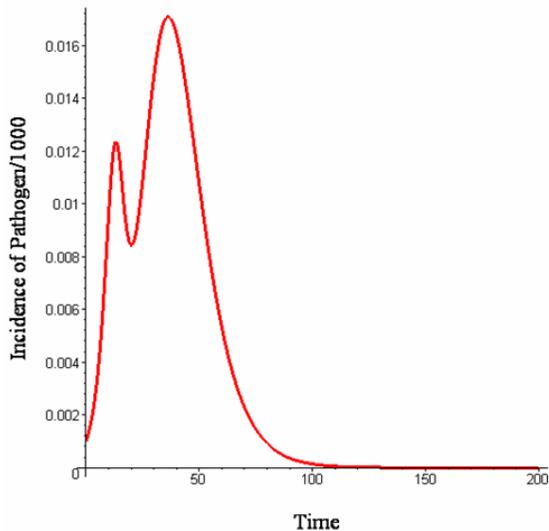

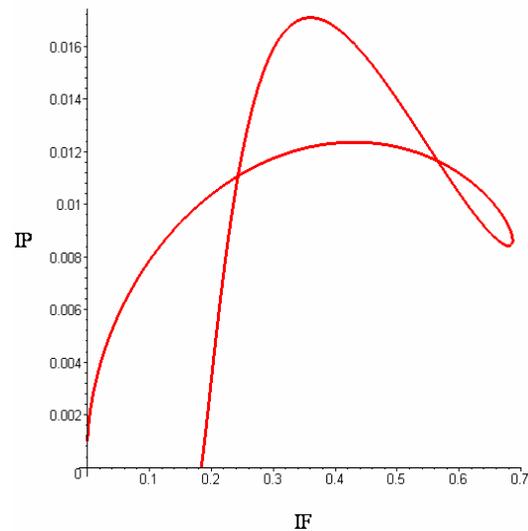**Figure 9a**: Incidence of Pathogen   **Figure 9b**: Phase Portrait

Here, we suggest that these patterns might be created purely by the endogenous interplay between the spread of the influenza virus and the spread of fear or behavioral adaptation to the virus, but in a simpler memory-less system quite different from that of Bootsma and Ferguson.

Exogenous Account in the Agent Model

Let us now extend the agent model above to give an alternative "Top-Down" account. In the agent model elaborated earlier, the infection proper was of type SI. Now let us make it a classic SIR disease. Scared agents, whether infected or not, withdraw from circulation with some probability (set at 0.8) throughout, and stay in "the basement" (i.e., in isolation) until government issues an "all clear." We assume that this is issued when prevalence falls below some threshold, measured (by the government) as the fraction infected (I/N).

Posit endogenous distancing due to fear, as before. But now assume that public health authorities announce "all clear" at a low *infection* level—let us say 0.5%. It is certainly understandable that 1918 authorities would make the assumption that once the infection level has fallen to one half of one percent, it is safe to lift the measures. But it was wrong. Multiple waves ensue, as shown in Run 5 (Figure 10).
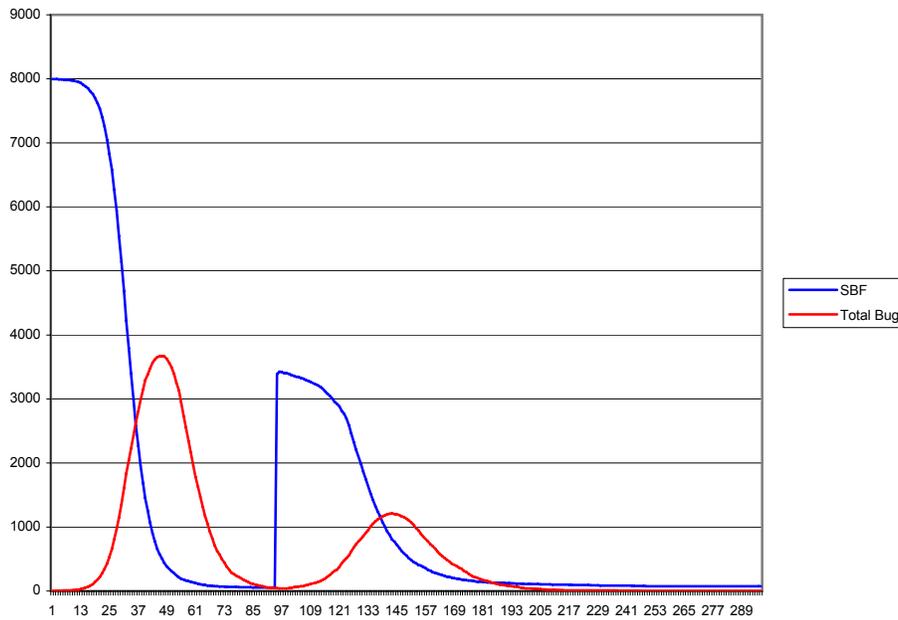
Figure 10*: Multiple waves.*

What explains this? The differential equations elaborated at the outset tell the essential story. Indeed the simplest version—the fear-free (β=0) Kermack-McKendrick Model gives the answer.

Authorities surmised that a low level of *infection* made it safe to relax distancing. But they lacked the central Kermack-McKendrick (1927) insight that it is *S*, not *I*, that is the epidemic threshold. For an SIR process, the condition for an epidemic to take off (i.e., for *dI/dt* to be positive) is, in fact, that the *susceptible* pool exceed the relative removal rate, λ/β. That is:

$$\frac{dI}{dt} = \beta SI - \lambda I > 0 \Leftrightarrow S > \frac{\lambda}{\beta} \quad [4]$$

In 1918, infection and distancing had reduced the susceptible pool *S* to sub-threshold, and *I* was indeed declining. But the abrupt release of susceptibles from isolation poured fuel on the infective embers, pushing S back over the threshold, producing a 2nd wave.

Summary on 1918 Temporal Waves

The present model can thus generate waves through decentralized (bottom up) behavioral adaptations or through centralized (top down) premature government relaxations of isolation. It may be that different mechanisms or mixes of them were at play in particular cases. Further research is surely warranted.

PART II. SPATIAL PROPAGATION:
THE EXTENDED AGENT MODEL WITH FLIGHT

As noted earlier, most research in epidemiology does not take into consideration the possibility of behavioral adaptations that are prevalence-dependent (see above). Those models that *do* include prevalence-dependent behavior almost exclusively assume behavioral changes that are *depressive* in their effect on the epidemic, protective self-isolation (sequestration) being the most common .

However, research on mass behavior during crises (and even epidemics specifically) records another behavioral response that is common—*flight*. Historical cases of flight from epidemics are numerous, dating back at least as far as Medieval Europe, where the morality of fleeing from the Plague was a central and divisive topic among early modern Jesuits (Martin 1996). In the 19th century, large scale flight was a common behavioral response to urban epidemics of cholera and yellow fever. For example, more than 25,000 residents (almost half the population) fled Memphis when yellow fever struck in summer 1878, and as the fever spread through the South the highest incidence was in cities directly along railroad lines leading out of Memphis (Tennessee Encyclopedia). Within days of cholera's appearance in Cairo in 1831, the Nile "swarmed with craft of every description filled with refugees from the stricken city" as a mass exodus began (Kuhnke 1990). Cholera arrived in North America for the first time in 1832, carried by Irish immigrants fleeing the epidemic in Ireland. As it spread rapidly through the Midwest and Northeast of the United States, flight was common: "the appearance of cholera in even the smallest hamlet was the signal for… headlong flight, spreading the disease throughout the surrounding countryside" (Rosenberg 1962). Flight was also a response to 20th century epidemics such as polio, influenza, and plague. In some cases, fear alone was sufficient to cause flight (even in the absence of any confirmed disease) and "sociogenic" illness—for example in Surat India in 2006, and Melbourne Australia in 2005 (Bartholomew and Wessely 2002, Bartholomew 2005, IANS 2006).

The potential for flight as a behavioral response to disease prevalence has important consequences for epidemic modeling. Unlike protective sequestration, flight has the potential to *increase* mixing in the short term, and across spatial regions (even if it ultimately removes individuals from circulation *locally*). In the model developed below, we expand the behavioral response repertoire of agents infected with fear to include both flight and protective self-isolation. For now, a specific behavioral response is a characteristic of each individual—some agents always flee when afraid, others hide. We explore the impact of differing levels of flight on the epidemic dynamics.

Set-up

The agent model with self-isolation and flight takes place on a 2D lattice. Each agent (except the infection seeding agent who starts in a corner) is given a

random initial location. Normally, agents move a short distance[5] each round in a random walk, and interact with a random agent in their vision (if any). Contact spreads both the bug and the fear according to α and β. However, once agents contract fear they may adapt their movement and contact behaviors.

The model has three types of agents, representing three different characteristic responses to fear. The first type, "fleers", respond to fear by selecting a distant location[6] on the lattice and moving directly to that location as fast as possible. Upon reaching the goal location this agent will recover from fear and his movement rule reverts to the random walk. The second type, "hiders", respond to fear by removing themselves from circulation for a specified number of iterations (during which they neither move nor contact other agents). The third type, "ignorers", never change their behavior and remain in normal circulation.

Parameters of the model include the movement and contact radii, the distribution of agents across the three types of behavioral responses, and the duration and transmission rates of fear and the bug[7].

Sensitivity to Flight

The results from this agent model highlight the importance of flight as an avenue for research—even a small amount of flight can have a dramatic impact on epidemic dynamics.

First, to establish a baseline, we consider the simple form of the model in which fear does not play a role—no one hides or flees. All agents are "ignorers". In a representative run (shown in Figure 11) the model produces standard SIR curves.
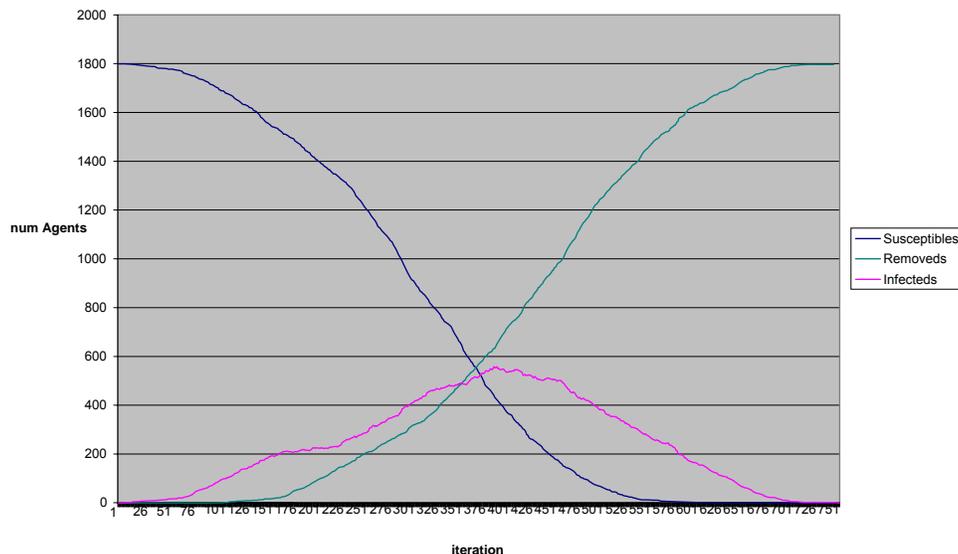

Figure 11: Standard SIR curves in a representative simulation run with all "ignorers"

[5] For the runs reported here, this is a random Moore neighboring site.
[6] For the runs reported here, this is a random site 15 sites south of the agent's current location.
[7] The parameters used for all of the simulation experiments discussed in this section, are: 1800 agents on a 120x120 lattice, alpha = 0.11, beta = 0.1, lambda = 0.015, illness duration = 100 periods, fear duration = 800 periods

In a 30-run analysis, the average epidemic duration with all agents set to "ignorers" is 742.1 periods (SE 9.5), and average total incidence is 99.9%. (See the leftmost bars of Figures 12a and b, respectively)

We now introduce the coupled epidemic of fear and disease, as described above—with only protective isolation allowed as a response to fear. This reduces incidence enormously (to an average of 27.8%) and stops the epidemic earlier (in an average of 647 rounds). See the middle bars of Figure 12a and b below.

Next, we introduce flight, but only a small amount—90% of agents still respond to fear by hiding (removing themselves from circulation), and only 10% flee. How does this small proportion of flight affect incidence and duration of the epidemic?
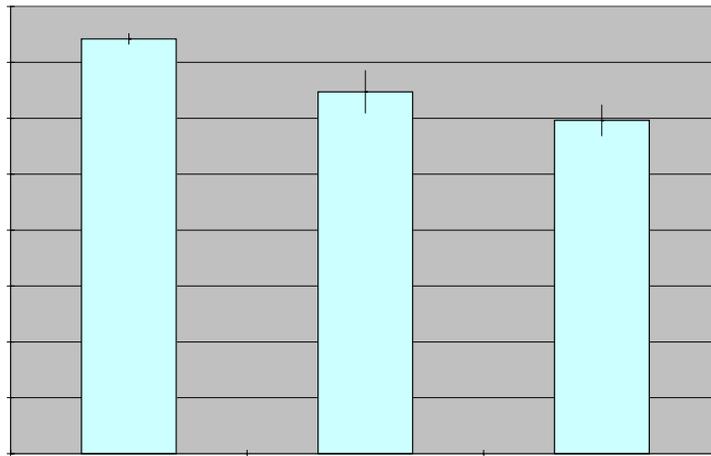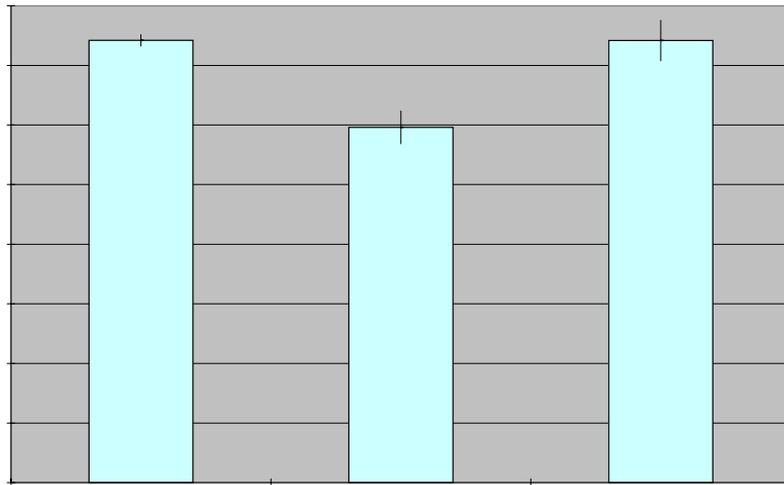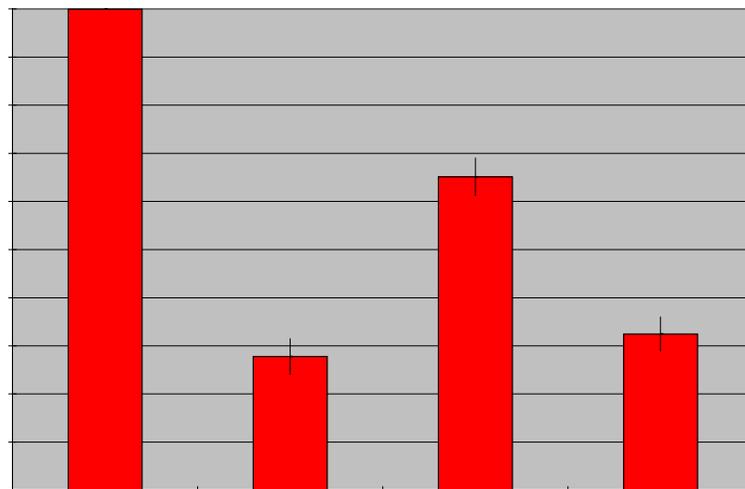

(12a)
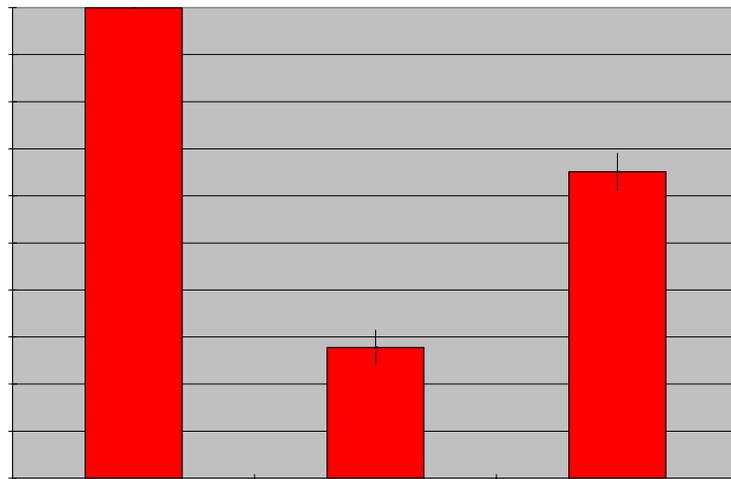
(12b)

Figure 12 (a & b): *Epidemic duration and total incidence under three different parameter settings. Each bar in the chart represents an average across 30 simulation runs for a given parameter setting, with standard error range. When all agents hide, the epidemic is shorter and has substantially lower incidence that with no adaptive behavior. When a small percentage of agents flee (with the majority hiding), however, incidence goes up substantially even as the duration falls farther.*

As Figure 12 above shows, even a small amount of flight has dramatically *increased* the spread of the epidemic—resulting in much higher overall incidence with a shorter duration (comparing the rightmost bars of 12a and b to the others).

Of course, the 10% of agents who are fleeing are also not hiding. By remaining in circulation, even non-fleeing non-hiders have an inflammatory effect on the epidemic. So is it the flight or simply the increased circulation from non-hiding which is driving the results shown in Figure 12? To answer this question, we ran the simulation with 90% "hiders" and 10% non-hiding, non-fleeing "ignorers". As Figure 13 illustrates, the results from these runs differ noticeably from the runs with actual flight—suggesting that flight has a substantial impact above and beyond increasing the number of "non-hiders".

(13a)

(13b)

Figure 13 (a & b): *A comparison of epidemic duration and total incidence with 10% "fleers" versus 10% "ignorers". As before, each bar in the chart represents an average across 30 simulation runs for a given parameter setting, with standard error range. The runs with 10% "ignorers" have similar incidence to runs with 100% "hiders", and similar duration to runs with*

16

100% "ignorers". By contrast, the runs with 10% "fleers" have much higher incidence and lower duration.

Not only does flight increase incidence dramatically, but it also increases the rapidity and geographic scope of the epidemic. One way to measure the geographic spread of the bug is to begin the epidemic with an index case in one corner of the 2D lattice, and observe if and when the bug reaches the far diagonal corner[8]. Figure 14 shows that epidemics rarely spread fully across the lattice with no flight—but almost always spread fully across the lattice with even a small amount of flight.
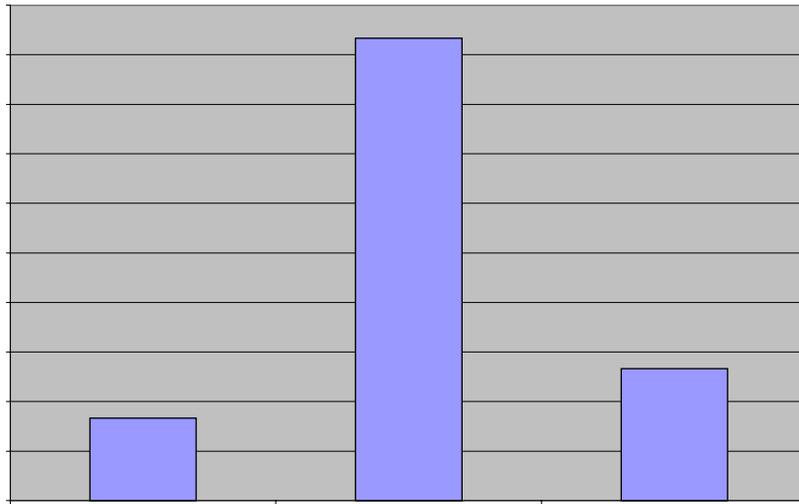

Figure 14: *The percentage of runs (out of 30) for each parameter setting in which the epidemic spreads fully across the landscape, from an index case in one corner of the lattice all the way to the opposite corner.*

Furthermore, in rare cases where the epidemic spreads fully across the lattice without flight, it takes much longer to do so than in cases with flight, as shown in Figure 15.

---

[8] Obviously, unlike the lattice with periodic boundary conditions used above to mimic the ODEs, this lattice is not a topological torus.
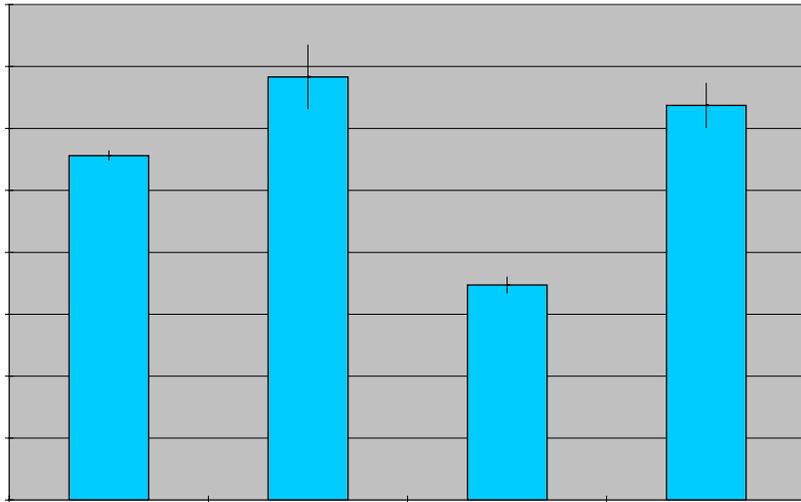
Figure 15: *Epidemic Spread Time (Runs with corner-to-corner spread).*

For an illustration of how flight spreads the epidemic quickly across the lattice, increasing both incidence and speed, see Figure 16 below. Blue dots represent susceptibles (infected with neither fear nor pathogen); yellow dots, infected with fear alone; orange dots, acting on fear; red dots, infected with pathogen; white dots, recovered. In the first screen shot (16a), with no flight, yellow agents (infected with fear) form a moving buffer zone between the epidemic of pathogen and the susceptible agents. Since the fear arrives first, agents can respond by removing themselves from circulation before they are infected with pathogen. In the second screen shot (16b), with a small amount of flight, a few infected fleeing agents pierce this buffer zone—moving the pathogen quickly into the susceptible pool.
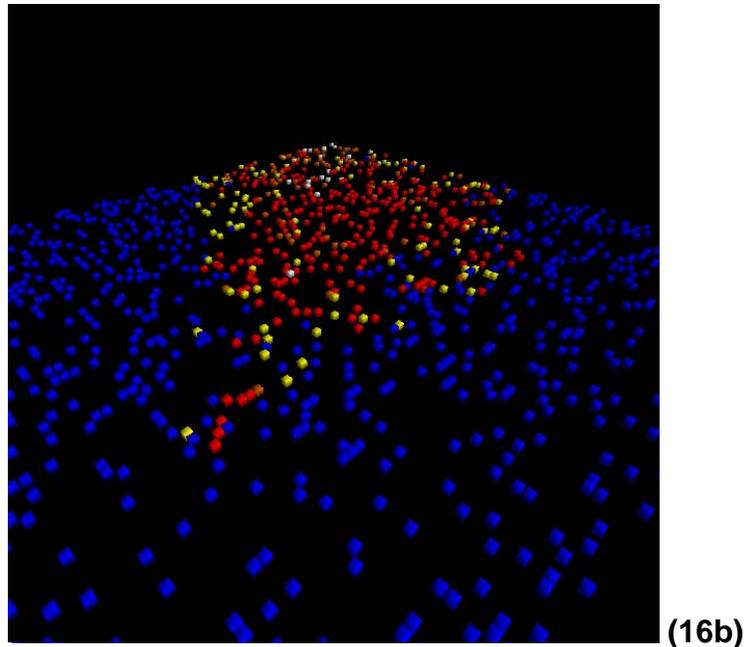

(16a)

(16b)
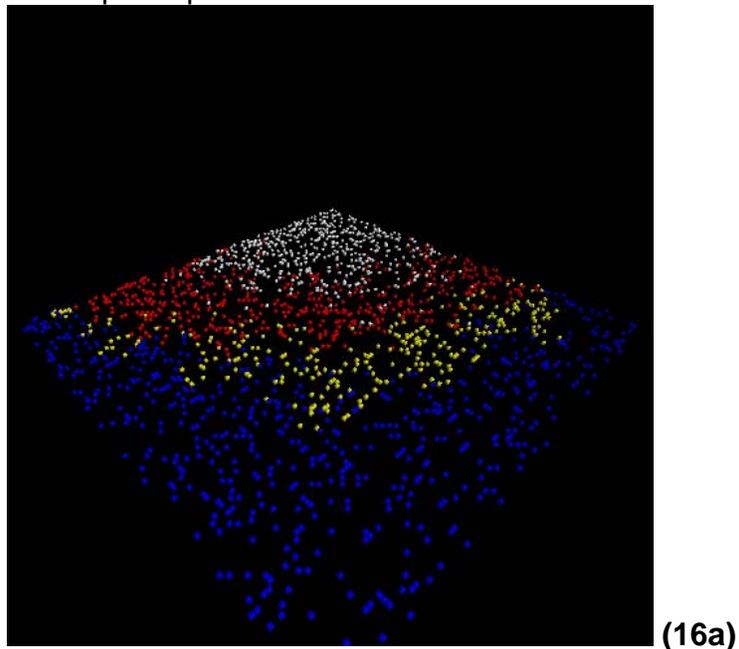
Figure 16 (a & b): Screenshots from the agent-based simulation model without and with flight. Each agent is represented by a colored dot on the lattice.

Conclusion

These specific quantitative results are, of course, dependent on the specific parameters used above. But the larger qualitative point is robust: "prevalence elastic" behavioral adaptation need not damp the force of an epidemic. If flight is admitted, this form of "social distancing" can amplify the contagion and spread it spatially. This exposition invites a great deal of further work, including development of the multi-patch ODEs with flight, full sensitivity analysis of the agent-based model, further "dialogue" between the two, and calibration to historical cases.

In general, this effort enforces the overarching point that *infectious disease models must incorporate behavior*. Indeed, the model—while explored for contagious disease here—can be applied to a wide range of cases where momentous contagions of fear eventuate from events that are not themselves contagious.

References

Anderson, R.M. and R.M. May. (1983). *Infectious Diseases of Humans*. Oxford, U.K.: Oxford Science Publications.

Auld, M. (2006). "Estimating Behavioral Response to the AIDS Epidemic." *Contributions to Economics Analysis & Policy, Vol. 5,* No. 1, pp. 1235-1235.

Bartholomew, R.E. (2005). "Mystery illness at Melbourne Airport: toxic poisoning or mass hysteria?" *Medical Journal of Australia, Vol. 183*, No. 11/12, pp. 564-566.

Bartholomew, R. E. and S Wessely. (2002). "Protean nature of mass sociogenic illness: From possessed nuns to chemical and biological terrorism fears." *The British Journal of Psychiatry, Vol. 180*, pp. 300-306.

Bootsma, M. and N Ferguson. (2007). "The effect of public health measures on the 1918 influenza pandemic in U.S. cities." *Proceedings of the National Academic of Sciences* 104: pp. 7588-7593.

Caplinger, C. (2002). "Yellow Fever Epidemics." *The Tennessee Encyclopedia of History and Culture*. 09 Oct 2007. <http://tennesseeencyclopedia.net/imagegallery.php?EntryID=Y002>.

Cockburn, P. "My legs and back became weaker; I found it difficult to sit up." *The Independent* (London) 5 Aug 2004.

Del Valle, S, H.W. Hethcote, J.M. Hyman, and C. Castillo-Chavez. (2005). "Effects of Behavioral Changes in a Smallpox Attack Model." *Mathematical Biosciences*, Vol. *195,* No. 2, pp. 228-251.

Diekman, O., J.A.P. Heesterbeek, and J.A.J. Metz. (1990). "On the definition and computation of the basic reproduction ratio R_0 in models of infectious diseases in heterogeneous populations." *Journal of Mathematical Biology, Vol. 28,* No. 4, pp. 365-283.

Kermack, W.O. and A. G. McKendrick. (1927). "A Contribution to the Mathematical Theory of Epidemics." *Proceedings of the Royal Society of London. Series A, Containing Papers of a Mathematical and Physical Character, Vol. 115*, No. 772, pp. 700-721.

Kremer, M. (1996). "Integrating behavioral choice into epidemiological models of the AIDS epidemic." *Quarterly Journal of Economics*, *Vol. 111,* No. 2, pp. 549-573.

Kuhnke, L. (1990). *Lives at Risk: Public Health in the Nineteenth-Century Egypt*. Berkeley, CA: University of California Press.

Martin, A. L. (1996). *Plague? Jesuit Accounts of Epidemic Disease in the Sixteenth Century*. Kirksville, MO: Sixteenth Century Journal Publishers.

Mullahy, J. (2000). "It'll only hurt a second? Microeconomics of who gets flu shots." *Health Economics*, *Vol.* 8, 9-24.

Murray, J.D. (1989). *Mathematical Biology. Biomathematics **19***. New York, NY: Springer-Verlag.

Philipson, T. (2000). "Economic epidemiology and infectious diseases," in A. Culyer and J. Newhouse (eds.), *Handbook of Health Economics*. Amsterdam, Netherlands: Elsevier North Holland.

Rosenberg, C. E. (1962*). The Cholera Years: The United States in 1832, 1849, and 1866.* Chicago, IL: University of Chicago Press.

Wilson, John L. (1999). *Stanford University School of Medicine and the Predecessor Schools: An Historical Perspective*. <http://elane.stanford.edu/wilson/index.html>.

Yue, Y, Cummings, DAT, Burke, DS, Louis TA. "Bayesian analysis of infectious disease time series data." In preparation.

Zabel, J. (1998). "An analysis of attrition in the Panel Study of Income Dynamics and the Survey of Income and Program Participation with an application to a model of labor market behavior." *Journal of Human Resources*, *Vol. 33*, No. 2, pp. 479–506.